IEEE Access
Multidisciplinary | Rapid Review | Open Access Journal

Received December 21, 2016; accepted January 4, 2017, date of publication January 16, 2017, date of current version March 6, 2017.

Digital Object Identifier 10.1109/ACCESS.2017.2651048

Convergence Analysis on Multi-AUV Systems With Leader-Follower Architecture

WEN XING[1], YUXIN ZHAO[1], (Senior Member, IEEE), AND HAMID REZA KARIMI[2], (Senior Member, IEEE)

[1]College of Automation, Harbin Engineering University, Harbin 150001, China
[2]Department of Mechanical Engineering, Politecnico di Milano, 20156 Milan, Italy

Corresponding author: Y. Zhao (zhaoyuxin@hrbeu.edu.cn)

This work was supported in part by the National Natural Science Foundation of China (51379049, 41676088), in part by the China Scholarship Council, in part by the Heilongjiang Youth Science Foundation under Grant QC2016082, and in part by the Alexander von Humboldt-Stiftung under Grant 1121070 STP.

ABSTRACT In multi-autonomous underwater vehicle (multi-AUV) systems, the convergence rate is characterized by the pace of consistency of the key state information for each member. The topology with leader–follower architecture is designed as a combination of an undirected graph between followers and a digraph between leaders and followers. An overview of influences on convergence rate of the second-order consensus algorithm is elaborated in three aspects, along with the main contributions in this paper. Specifically, the explicit expression of the maximum convergence rate is established based on the root locus method, and then, the effects of control parameters on the convergence rate are analyzed. Moreover, the influences of network topologies on the convergence rate are investigated from the view of adjusting the existing connectivity, changing the weights on links, and utilizing hierarchical structure. The combination of consensus and filtering algorithm is also an approach to enhance the capacity of multi-AUV systems. In order to eliminate the accumulated errors in the process of dead reckoning, a collaborative navigation model is presented, and then, a localization approach based on consensus-unscented particle filter algorithm is proposed. Simulations results are provided to verify location performance under the assumption of Gaussian white noise in the systems. In addition, the influences of the topologies on positioning accuracy are explored.

INDEX TERMS Multi-AUV systems, network topology, second-order consensus algorithm, convergence rate, consensus-UPF algorithm.

I. INTRODUCTION

Enlightened by cooperative behaviors in nature, such as migration of birds in groups, synchronous luminescence of fireflies, foraging of schools of fish and so force, the cooperative control problems have attracted more and more attentions. The specific examples of agents contain satellites, robots, unmanned aerial vehicles, wireless sensors and autonomous underwater vehicles. Multi-agent system, as the name implies, is a network system which is composed of some intelligent agents with independent capacities.

The ability of a single agent is considerably limited and unable to meet the demands under complicated and changeable environment, while multi-agent systems concentrate on the close cooperation between members, rather than autonomy and exertion of individual capacity. It is an undeniable fact that its actual applications in solving large, complex problems are of great advantages. In intelligent robot systems, individual agent should include some information processing subsystems, such as visual information processing module, data fusion module, planning and decision-making module as well as autopilot and so on. The overall mission is effectively completed by the interdependent and inter-prerequisite subsystems via sharing the information and mutual coordination. In terms of transportation, due to the distributed characteristics of traffic network, especially for the unpredictable traffic conditions when the accident occurred, distributed cooperative control protocols are more suitable for traffic control. In the industrial field, multi-agent systems with relatively higher efficiency are sometimes substituted for workers to finish massive production and cargo transportation in the adverse operation circumstances. For entertainment, multiple soccer robot systems can adopt a valid distributed control

algorithm and maintain or dynamically switch a proper geometric pattern to meet tactical demands. Proper formation topology is beneficial for exchanging information rapidly and accurately.

As to multi-agent cooperative control, it is difficult to obtain other members' key information for each single member due to the communication constraints. This means that each individual agent lakes global knowledge of the whole system. In order to ensure the normalized operation and satisfactory performance, the distributed cooperative control strategy based on local information exchange is generally adopted so that agent can interact with its neighbors to achieve certain global behaviors. With this framework, communication graph and consensus protocol, which determine what information is available and how the information propagates for each agent at each time instant, are significant aspects in distributed coordination. More specifically, in specific distributed control structure, each agent has its relatively independent information such as position, velocity, attitude and target, and meanwhile exchanges required information with neighbor agents. Its final trajectory is determined by the interaction of these two kinds of information. Note that algebraic graph theory pertains to tackle the problems about graph by utilizing algebraic properties of graph. In this paper, an algebraic graph theory is devoted to delineate the interior connection of multi-agent systems. Agents and communication links are regarded as notes and edges in graph respectively so as to establish graph theory model. In this way, researches on consensus performance rely on the exploration of eigenvalues of graph Laplacian to a great extent. One performance index of consensus algorithm is convergence speed, which depicts how fast the individual agents achieve an agreement and serve as important design consideration for multi-agent systems. Approaches causing a rapid convergence rate of consensus algorithm are summarized in the following two aspects. 1) One way is to design the suitable weights or topology of network to get a relatively high algebraic connectivity. Thus more adequate information exchange will accelerate the convergence speed. 2) An alternative way is that effective control strategy contributes to fast consensus. Influences on the convergence rate to consensus will be further analyzed in this paper.

In this paper, more backgrounds on the application of multi-agent systems are summarized. As an important application, graph theory model of multi-AUV systems with leader-follower architecture based on second-order consensus algorithm is presented in Section 1. The model of AUV is relatively simple under the large scale, and all-actuated AUV can be simplified and formalized as the second-order integrator. Moreover, eigenvalues of Laplacian of the whole network graph are solved as significant parameters for the analysis on convergence rate. Overview of approaches to accelerate the convergence rate of consensus algorithm is discussed in different cases in following sections, containing the design of control protocols, the improvement of network topology and the combination of consensus algorithm and other effective algorithms such as filtering algorithm.

The main contributions in this paper are added in each part. In Section 2, we discussed the influences of two control gains on the maximum convergence rate which is expressed explicitly by the root locus method. In Section 3, effects of adjusting the nodes, edges and weights on convergence rate to consensus are demonstrated. In order to further improve the performance of multi-AUV systems, the collaborative model is built and a collaborative navigation algorithm based on consensus-UPF algorithm is proposed in Section 4. Relevant simulations are designed to illustrate the influences of topologies on positioning accuracy when carrying out the collaborative navigation tasks. Finally, concluding remarks are made in Section 5.

A. GRAPH THEORY MODEL BASED ON SECOND-ORDER CONSENSUS

Consensus algorithms refer to that each agent of multi-AUV systems gradually converges to a consistent state with the mutual exchange of the key information under the given initial state and a period of movement. In order to implement the stable formation, the uniform convergence rate, the desirable distances to the determined neighbors and the target location are required for each AUV, which means that the control protocol is a function composed by speed difference, position difference and target location. In the leader-follower architecture, the key information of every follower tends to that of a leader or to the region formed by leaders eventually. If the dynamic characteristics of leaders are linear functions changed over time, all the final states of followers in multi-AUV systems are linear. This is the notion about linear consensus. What calls for special attention is that the state of leaders is known, and leaders mainly provide referable control instructions for followers which are unable to obtain the information from neighbor AUVs. We defined that the whole network graph G is made up of the topology G_{ff} between followers and the topology G_{lf} between followers and leaders. G_{lf} is a digraph because the information transmission between leaders and followers is unidirectional. In this paper, we assume that the graph G_{ff} is an undirected graph.

Consider a group of leader agents with the following dynamics:

$$\begin{cases} \dot{\xi}_j^L = \zeta_j^L \\ \dot{\zeta}_j^L = u_j^L \end{cases}$$

where ξ_j^L is the position, ζ_j^L $(j = 1, \ldots, m)$ is the velocity and u_j^L represents the control input of j-th leader.

As above, the dynamic characteristics of followers are described as the second-order integrator structures:

$$\begin{cases} \dot{\xi}_i^F = \zeta_i^F \\ \dot{\zeta}_i^F = u_i^F \end{cases} \tag{1}$$

where ξ_i^F is the position, ζ_i^F $(i = 1, \ldots, n)$ is the velocity and u_i^F represents the acceleration of i-th follower.

The consensus algorithm is selected as:

$$\begin{aligned}\dot{\zeta}_i^F &= u_i^F \\ &= -\sum_{j=1, j\in G_{ff}}^{n} a_{ij}\left[\gamma_0\left(\xi_i^F - \xi_j^F\right) + \gamma_1\left(\zeta_i^F - \zeta_j^F\right)\right] \\ &\quad -\sum_{j=1, j\in G_{lf}}^{m} d_{ij}\left[\gamma_0\left(\xi_i^F - \xi_j^L\right) + \gamma_1\left(\zeta_i^F - \zeta_j^L\right)\right] \quad (2)\end{aligned}$$

where a_{ij} is the (i, j)-th element of adjacent matrix A, denoting communication weights between followers. d_{ij} represents the status of communication between leaders and followers. If there is an edge between leader and follower, it means that d_{ij} is equal to the value of weight on the edge. If the edge is going from j to i, then $a_{ij} \neq 0$, $d_{ij} \neq 0$. Our paper focuses on the consensus protocol with time-invariant parameters of topology, thus A is the constant matrix, $a_{ij} \in R^+$, $d_{ij} \in R^+$ and $\gamma_0, \gamma_1 \in R$. In (1),

$$-\sum_{j=1, j\in G_{ff}}^{n} a_{ij}\left[\gamma_0\left(\xi_i^F - \xi_j^F\right) + \gamma_1\left(\zeta_i^F - \zeta_j^F\right)\right]$$

imposes effects on trajectories of followers to let them reach unanimity, and

$$-\sum_{j=1, j\in G_{lf}}^{m} d_{ij}\left[\gamma_0\left(\xi_i^F - \xi_j^L\right) + \gamma_1\left(\zeta_i^F - \zeta_j^L\right)\right]$$

is regarded as a pinning control, making the trajectories of followers closer to that of leaders.

For each follower, (1) and (2) can be replaced by:

$$\begin{aligned}\dot{\xi}_1^F &= \zeta_1^F \\ &\vdots \\ \dot{\xi}_n^F &= \zeta_n^F \\ \dot{\zeta}_1^F &= -\gamma_0\begin{bmatrix}(a_{12}+\cdots+a_{1n}+d_{11}+\cdots+d_{1m})\,\xi_1^F \\ -a_{12}\xi_2^F - \cdots - a_{1n}\xi_n^F - d_{11}\xi_1^L - \cdots \\ -d_{1m}\xi_m^L\end{bmatrix} \\ &\quad -\gamma_1\begin{bmatrix}(a_{12}+\cdots+a_{1n}+d_{11}+\cdots+d_{1m})\,\zeta_1^F \\ -a_{12}\zeta_2^F - \cdots - a_{1n}\zeta_n^F - d_{11}\zeta_1^L - \cdots \\ -d_{1m}\zeta_m^L\end{bmatrix} \\ &\vdots \\ \dot{\zeta}_n^F &= -\gamma_0\begin{bmatrix}\left(a_{n1}+\cdots+a_{n,n-1}+d_{n1}+\cdots+d_{nm}\right)\xi_n^F \\ -a_{n1}\xi_1^F - \cdots - a_{n,n-1}\xi_{n-1}^F - d_{n1}\xi_1^L - \cdots \\ -d_{nm}\xi_m^L\end{bmatrix} \\ &\quad -\gamma_1\begin{bmatrix}\left(a_{n1}+\cdots+a_{n,n-1}+d_{n1}+\cdots+d_{nm}\right)\zeta_n^F \\ -a_{n1}\zeta_1^F - \cdots - a_{n,n-1}\zeta_{n-1}^F - d_{n1}\zeta_1^L - \cdots \\ -d_{nm}\zeta_m^L\end{bmatrix}\end{aligned}$$

Select $\mathcal{X}^F = \left[\xi_1^F, \ldots, \xi_n^F, \zeta_1^F, \ldots, \zeta_n^F\right]^T$ as state and then:

$$\begin{aligned}\dot{\mathcal{X}}^F &= \begin{bmatrix}0_{n\times n} & I_n \\ -\gamma_0\left(L+\tilde{D}\right)_{n\times n} & -\gamma_1\left(L+\tilde{D}\right)_{n\times n}\end{bmatrix}\mathcal{X}^F \\ &\quad + \begin{bmatrix}0_{n\times m} & 0_{n\times m} \\ \gamma_0 D_{n\times m} & \gamma_1 D_{n\times m}\end{bmatrix}\mathcal{X}^L \quad (3)\end{aligned}$$

where

$$\begin{aligned}\mathcal{X}^F &= \left[\xi_1^F, \ldots, \xi_n^F, \zeta_1^F, \ldots, \zeta_n^F\right]^T \\ \mathcal{X}^L &= \left[\xi_1^L, \ldots, \xi_m^L, \zeta_1^L, \ldots, \zeta_m^L\right]^T \\ L &= \left[l_{ij}\right]_{n\times n}, \quad l_{ii} = \sum_{j=1, j\neq i}^{n} a_{ij}, \quad l_{ij} = -a_{ij}\,(i \neq j) \\ D &= \left[d_{ij}\right]_{n\times m}, \quad \tilde{D} = diag\left(\sum_{i=1}^{m} d_{1i}, \sum_{i=1}^{m} d_{2i}, \ldots, \sum_{i=1}^{m} d_{ni}\right)\end{aligned}$$

B. ANALYSIS ON EIGENVALUES OF GRAPH LAPLACIAN

Let

$$H = L + \tilde{D}, \quad \Theta = \begin{bmatrix}0_{n\times n} & I_{n\times n} \\ -\gamma_0 H & -\gamma_1 H\end{bmatrix}$$

and

$$B = \begin{bmatrix}0_{n\times m} & 0_{n\times m} \\ \gamma_0 D_{n\times m} & \gamma_1 D_{n\times m}\end{bmatrix}.$$

Then, (3) can be redefined as $\dot{X}(t) = \Theta X(t) + BU(t)$ under the noise environment, and its solution is as follows:

$$X(t) = e^{\Theta t}X(0) + \int_0^t e^{\Theta(t-\tau)}BU(\tau)\,d\tau \quad (4)$$

From the second term of (4), we have:

$$\begin{aligned}&\int_0^t e^{\Theta(t-\tau)}BU(\tau)\,d\tau \\ &= \int_0^t e^{\Theta(t-\tau)}B\begin{bmatrix}\zeta_1^L(0)\,\tau + \frac{1}{2}a_1^L\tau^2 \\ \vdots \\ \zeta_m^L(0)\,\tau + \frac{1}{2}a_m^L\tau^2 \\ \zeta_1^L(0) + a_1^L\tau \\ \vdots \\ \zeta_m^L(0) + a_m^L\tau\end{bmatrix}d\tau \\ &= -\Theta^{-1}\left(\int_0^t B\begin{bmatrix}\zeta_1^L(0)\,\tau + \frac{1}{2}a_1^L\tau^2 \\ \vdots \\ \zeta_m^L(0)\,\tau + \frac{1}{2}a_m^L\tau^2 \\ \zeta_1^L(0) + a_1^L\tau \\ \vdots \\ \zeta_m^L(0) + a_m^L\tau\end{bmatrix}de^{\Theta(t-\tau)}\right)\end{aligned}$$

$$= -\Theta^{-1}\left(\begin{array}{l} e^{\Theta(t-\tau)}B\left[\begin{array}{c} \zeta_1^L(0)\,\tau+\frac{1}{2}a_1^L\tau^2 \\ \vdots \\ \zeta_m^L(0)\,\tau+\frac{1}{2}a_m^L\tau^2 \\ \zeta_1^L(0)+a_1^L\tau \\ \vdots \\ \zeta_m^L(0)+a_m^L\tau \end{array}\right]\Big|_0^t \\ -\int_0^t e^{\Theta(t-\tau)}Bd\left[\begin{array}{c} \zeta_1^L(0)\,\tau+\frac{1}{2}a_1^L\tau^2 \\ \vdots \\ \zeta_m^L(0)\,\tau+\frac{1}{2}a_m^L\tau^2 \\ \zeta_1^L(0)+a_1^L\tau \\ \vdots \\ \zeta_m^L(0)+a_m^L\tau \end{array}\right] \end{array}\right)$$

$$= -\Theta^{-1}\, e^{\Theta(t-\tau)}B\left[\begin{array}{c} \zeta_1^L(0)\,\tau+\frac{1}{2}a_1^L\tau^2 \\ \vdots \\ \zeta_m^L(0)\,\tau+\frac{1}{2}a_m^L\tau^2 \\ \zeta_1^L(0)+a_1^L\tau \\ \vdots \\ \zeta_m^L(0)+a_m^L\tau \end{array}\right]\Big|_0^t$$

$$-\left(\Theta^{-1}\right)^2 e^{\Theta(t-\tau)}B\left[\begin{array}{c} \zeta_1^L(0)+a_1^L\tau \\ \vdots \\ \zeta_m^L(0)+a_m^L\tau \\ a_1^L \\ \vdots \\ a_m^L \end{array}\right]\Big|_0^t$$

$$-\left(\Theta^{-1}\right)^3 e^{\Theta(t-\tau)}B\left[\begin{array}{c} a_1^L \\ \vdots \\ a_m^L \\ 0_{m\times 1} \end{array}\right]\Big|_0^t$$

$$= -\Theta^{-1}B\left[\begin{array}{c} \zeta_1^L(0)\,t+\frac{1}{2}a_1^Lt^2 \\ \vdots \\ \zeta_m^L(0)\,t+\frac{1}{2}a_m^Lt^2 \\ \zeta_1^L(0)+a_1^Lt \\ \vdots \\ \zeta_m^L(0)+a_m^Lt \end{array}\right] + \Theta^{-1}e^{\Theta t}B\left[\begin{array}{c} 0_{m\times 1} \\ \zeta_1^L \\ \vdots \\ \zeta_m^L \end{array}\right]$$

$$-\left(\Theta^{-1}\right)^2 B\left[\begin{array}{c} \zeta_1^L(0)+a_1^Lt \\ \vdots \\ \zeta_m^L(0)+a_m^Lt \\ a_1^L \\ \vdots \\ a_m^L \end{array}\right] + \left(\Theta^{-1}\right)^2 e^{\Theta t}B\left[\begin{array}{c} \zeta_1^L(0) \\ \vdots \\ \zeta_m^L(0) \\ a_1^L \\ \vdots \\ a_m^L \end{array}\right]$$

$$-\left(\Theta^{-1}\right)^3 B\left[\begin{array}{c} a_1^L \\ \vdots \\ a_m^L \\ 0_{m\times 1} \end{array}\right] + \left(\Theta^{-1}\right)^3 e^{\Theta t}B\left[\begin{array}{c} a_1^L \\ \vdots \\ a_m^L \\ 0_{m\times 1} \end{array}\right]$$

where

$$\Theta^{-1}B = \left[\begin{array}{cc} -H^{-1}D & -\frac{\gamma_1}{\gamma_0}H^{-1}D \\ 0_{n\times m} & 0_{n\times m} \end{array}\right]$$

$$\left(\Theta^{-1}\right)^2 B = \left[\begin{array}{cc} \frac{\gamma_1}{\gamma_0}H^{-1}D & \frac{\gamma_1^2}{\gamma_0^2}H^{-1}D \\ -H^{-1}D & -\frac{\gamma_1}{\gamma_0}H^{-1}D \end{array}\right]$$

$$\left(\Theta^{-1}\right)^3 B = \left[\begin{array}{cc} \left(\begin{array}{c} -\frac{\gamma_1^2}{\gamma_0^2}H^{-1}D \\ +\frac{1}{\gamma_0}\left(H^{-1}\right)^2D \end{array}\right) & \left(\begin{array}{c} -\frac{\gamma_1^3}{\gamma_0^3}H^{-1}D \\ +\frac{1}{\gamma_1}\left(H^{-1}\right)^2D \end{array}\right) \\ \frac{\gamma_1}{\gamma_0}H^{-1}D & \frac{\gamma_1^2}{\gamma_0^2}H^{-1}D \end{array}\right]$$

If all the eigenvalues of Θ have the negative real parts and $t \to \infty$, the states of followers converge to the linear combination of the states of leaders finally.

$$\left[\xi_1^F(t),\ldots,\xi_n^F(t)\right]^T$$

$$\to H^{-1}D\left[\begin{array}{c} \zeta_1^L(0)\,t+\frac{1}{2}a_1^Lt^2 \\ \vdots \\ \zeta_m^L(0)\,t+\frac{1}{2}a_m^Lt^2 \end{array}\right] - \frac{1}{\gamma_0}\left(H^{-1}\right)^2D\left[\begin{array}{c} a_1^L \\ \vdots \\ a_m^L \end{array}\right]$$

$$\to H^{-1}D\left[\begin{array}{c} \xi_1^L(t) \\ \vdots \\ \xi_m^L(t) \end{array}\right] - \frac{1}{\gamma_0}\left(H^{-1}\right)^2D\left[\begin{array}{c} a_1^L \\ \vdots \\ a_m^L \end{array}\right]$$

$$\left[\zeta_1^F(t),\ldots,\zeta_n^F(t)\right]^T$$

$$\to H^{-1}D\left[\begin{array}{c} \zeta_1^L(0)+a_1^Lt \\ \vdots \\ \zeta_m^L(0)+a_m^Lt \end{array}\right]$$

$$\to H^{-1}D\left[\begin{array}{c} \zeta_1^L(t) \\ \vdots \\ \zeta_m^L(t) \end{array}\right]$$

Next, we intend to solve equation $\det(\lambda I_{2n\times 2n}-\Theta)=0$ and evaluate the eigenvalues of Θ, because they will be used in the next section.

G_{ff} is an undirected graph, so it is easy to know that L is a symmetric matrix according to Lemma 1. Thus, H is a symmetric matrix because of the symmetry of matrix $\tilde{D}$, and then H is a Hermite matrix. Assume that diagonal matrix $\Lambda = diag(\mu_1,\mu_2,\ldots,\mu_n)$ is a production of eigenvalues of H, and then a unitary matrix must exist to prove the validity of $HU = U\Lambda$.

$$\begin{aligned} &\det(\lambda I_{2n\times 2n}-\Theta) \\ &\quad = \det\left(\left[\begin{array}{cc} \lambda I_{n\times n} & -I_{n\times n} \\ \gamma_0 H & \lambda I_{n\times n}+\gamma_1 H \end{array}\right]\right) \\ &\quad = \det\left[\lambda^2 I_{n\times n}+\gamma_1\lambda H+\gamma_0 H\right] \\ &\quad = \det\left[U^{-1}\left(\lambda^2 I_{n\times n}+\gamma_1\lambda H+\gamma_0 H\right)U\right] \end{aligned}$$

$$= \det\left[\lambda^2 I_{n\times n} + \gamma_1 \lambda U^{-1} H U + \gamma_0 U^{-1} H U\right]$$
$$= \det\left[\lambda^2 I_{n\times n} + \gamma_1 \lambda \Lambda + \gamma_0 \Lambda\right] \quad (5)$$
$$\det(\lambda I_n + H) = \prod_{i=1}^{n} (\lambda - \mu_i) \quad (6)$$

where μ_i is the i-th eigenvalue of H. By substituting (6) into (5), we can obtain:

$$\det\left[\lambda^2 I_{n\times n} + \gamma_1 \lambda \Lambda + \gamma_0 \Lambda\right] = \prod_{i=1}^{n} \left(\lambda^2 + \gamma_1 \mu_i \lambda + \gamma_0 \mu_i\right)$$
$$\det(\lambda I_{2n} - \Theta) = \prod_{i=1}^{n} \left(\lambda^2 + \gamma_1 \mu_i \lambda + \gamma_0 \mu_i\right) = 0$$
$$\lambda^2 + \gamma_1 \mu_i \lambda + \gamma_0 \mu_i = 0$$
$$\lambda_{i_1} = \frac{-\gamma_1 \mu_i + \sqrt{\gamma_1^2 \mu_i^2 - 4\gamma_0 \mu_i}}{2}$$
$$\lambda_{i_2} = \frac{-\gamma_1 \mu_i - \sqrt{\gamma_1^2 \mu_i^2 - 4\gamma_0 \mu_i}}{2} \quad (7)$$

From (7), it can be seen that the values of λ_{i_1} and λ_{i_2} (the eigenvalues of H) are related to μ_i (the eigenvalue of Θ). This means that λ_{i_1} and λ_{i_2} have strong associations with the eigenvalues of L.

II. THE INFLUENCES OF CONTROLLER DESIGN ON CONVERGENCE RATE

When designing the control strategies for multi-agent systems, some novel ideas are established by, for instance, utilizing the neighbor agents' past or current key information, choosing the proper control gains, introducing the past state into the current state for each agent and considering the constrains in practice. These approaches can cause each agent to obtain sufficient and effective information for improving the convergence speed of consistency.

In [1], multi-hop relay protocol was proposed in which each agent can expand the obtained information from neighbors' states by multi-hop paths. This method combined the key information of neighbor agents and their neighbors, so that each agent got more sufficient information and improved algebraic connectivity of network graph without changing the topological structure and then accelerated the convergence rate. The work in [2] decomposed the problem of seeking the fastest convergence rate of second-order consensus protocol with communication delay into two optimization problems to find optimal network topology and consensus gain by the root locus method in the frequency domain. When the topology cannot be reconstructed, the proposed method in [1] was extended to the time delay case to achieve the fastest convergence speed. A distributed consensus algorithm utilizing both the current states and the outdated states stored in memory was discussed in [3]. This method provided a faster convergence rate than the standard consensus algorithm. The results were generalized to discrete systems in [4]. In [5], a consensus control scheme was introduced. It relied on the average information of the agents' states in a certain time interval which was regarded as a more useful package of information to estimate next state. Furthermore, it was shown that a faster consensus was achieved if the time interval was proper. In [6]–[7], stability and parameter convergence of a distributed adaptive neural networks-based controller were analyzed under the assumption that each follower had a complete unknown controlling effect which depended on state, and the leader gave its commands only to a small portion of the graph. In the presence of external disturbances, a distributed finite-time observer was developed for guaranteeing that the state of the followers could converge to the convex hull spanned by those of the leaders in [8]. In [9], the disturbance rejection performance could be enhanced by adjusting the fractional power in the non-smooth controller, and the steady-state errors could reach a small region around the origin. In addition, the formation control in stealth with some restrictions was discussed in [10]–[11], tracking control of multi-agent systems with multiple delays and time-varying impulses was investigated in [12], a finite-time distributed $L_2 - L_\infty$ consensus protocol of networks with uncertain parameters was researched in [13], and the leader-following consensus for discrete-time directed networks with time delays and stochastic communication links was discussed in [14]. Distributed observer-type containment protocols and pinning synchronization problems for switching directed topologies were proposed in [15] and [16] respectively. In [17], containment control for second-order linear systems with leader-following framework under the sensor-to-controller delay and the controller-to-actuator delay was investigated. Based on Lyapunov stability theory and linear matrix inequality method, a sufficient condition of containment control was derived, which meant that all followers' states asymptotically converged to the convex hull spanned by the leaders'. In [18], an observer-based consensus control protocol for a series of L-order integrators with leader-following architecture was proposed, in which the time-varying delays and random packet dropouts were taken into consideration. Then, a new Lyapunov function was established for stability analysis. On the premise of stability, the suggested observer-type consensus was proved to accelerate the agreement between followers and leader. In addition, more novel control strategies and performance analysis for Roesser systems were provided in [19]–[21].

In this paper, the influences of control gains on convergence rate of second-order consensus algorithm are analyzed in following subsections. In order to obtain the expression of maximum convergence rate, we study root locus of the equation $\lambda^2 + \gamma_1 \mu \lambda + \gamma_0 \mu = 0$ under two conditions. If the farther closed-loop poles are from the imaginary axis, the shorter system response time is, and the faster the attenuation is. It implies that the exponential convergence rate is

$c(\gamma_1) = -\max\{\mathrm{Re}\lambda_{ij}, i = 1, 2, \ldots, n, j = 1, 2\}$. Since $\mathrm{Re}\lambda_{i1} \geq \mathrm{Re}\lambda_{i2}$ $(i = 1, 2, \ldots, n)$, λ_{i1} $(i = 1, 2, \ldots, n)$ is only for discussion when analyzing the maximum system convergence rate.

A. THE INFLUENCES OF γ_0 ON THE MAXIMUM CONVERGENCE RATE

Three lemmas are given and proved as follows:

Lemma 1: For the undirected graph $G = (V, \varepsilon, A)$, L is a symmetric matrix with some real eigenvalues, and the set of these eigenvalues can be ordered sequentially in an increasing order as [22]:

$$0 = \tilde{\mu}_1 \leq \tilde{\mu}_2 \leq \tilde{\mu}_3 \leq \cdots \leq \tilde{\mu}_n$$

where $\tilde{\mu}_i$ is the i-th eigenvalue of L and $\tilde{\mu}_2$ is the algebraic connectivity. $\tilde{\mu}_2 > 0$ if graph $G = (V, \varepsilon, A)$ is connected.

Lemma 2: Assume that $\mu_l > \mu_k > 0$, $\gamma_1 > 0$ and $\gamma_0 > 0$. (i) If $\gamma_0 < \frac{\gamma_1^2\mu_k}{4} < \frac{\gamma_1^2\mu_l}{4}$, then $\lambda_{l1}(\gamma_1)$ and $\lambda_{k1}(\gamma_1)$ are the complex numbers, and $\mathrm{Re}\lambda_{l1}(\gamma_1) < \mathrm{Re}\lambda_{k1}(\gamma_1)$; and
(ii) If $\gamma_0 \geq \frac{\gamma_1^2\mu_l}{4} > \frac{\gamma_1^2\mu_k}{4}$, then $\lambda_{l1}(\gamma_1)$ and $\lambda_{k1}(\gamma_1)$ are real numbers, and $\lambda_{l1}(\gamma_1) > \lambda_{k1}(\gamma_1)$.

Proof: (i) Put $\gamma_0 < \frac{\gamma_1^2\mu_k}{4} < \frac{\gamma_1^2\mu_l}{4}$ in formula

$$\lambda_{i1} = \frac{-\gamma_1\mu_i + \sqrt{\gamma_1^2\mu_i^2 - 4\gamma_0\mu_i}}{2},$$

we can get that:

$$\gamma_1^2\mu_l^2 - 4\gamma_0\mu_l < \frac{4\gamma_0}{\mu_l}\mu_l^2 - 4\gamma_0\mu_l = 0$$
$$\gamma_1^2\mu_k^2 - 4\gamma_0\mu_k < \frac{4\gamma_0}{\mu_k}\mu_k^2 - 4\gamma_0\mu_k = 0$$
$$\mathrm{Re}\lambda_{l1}(\gamma_1) = -\frac{\gamma_1\mu_l}{2} < -\frac{\gamma_1\mu_k}{2} = \mathrm{Re}\lambda_{k1}(\gamma_1)$$

(ii) Put $\gamma_0 \geq \frac{\gamma_1^2\mu_l}{4} > \frac{\gamma_1^2\mu_k}{4}$ in formula

$$\lambda_{i1} = \frac{-\gamma_1\mu_i + \sqrt{\gamma_1^2\mu_i^2 - 4\gamma_0\mu_i}}{2},$$

then, it follows:

$$\gamma_1^2\mu_l^2 - 4\gamma_0\mu_l \geq \frac{4\gamma_0}{\mu_l}\mu_l^2 - 4\gamma_0\mu_l \geq 0$$
$$\gamma_1^2\mu_k^2 - 4\gamma_0\mu_k \geq \frac{4\gamma_0}{\mu_k}\mu_k^2 - 4\gamma_0\mu_k \geq 0$$
$$\lambda_{l1} - \lambda_{k1} = \frac{-\gamma_1\mu_l + \sqrt{\gamma_1^2\mu_l^2 - 4\gamma_0\mu_l}}{2} - \frac{-\gamma_1\mu_k + \sqrt{\gamma_1^2\mu_k^2 - 4\gamma_0\mu_k}}{2}$$
$$= \frac{2\gamma_0\mu_l}{-\gamma_1\mu_l - \sqrt{\gamma_1^2\mu_l^2 - 4\gamma_0\mu_l}} - \frac{2\gamma_0\mu_k}{-\gamma_1\mu_k - \sqrt{\gamma_1^2\mu_k^2 - 4\gamma_0\mu_k}}$$
$$= \frac{2\gamma_0}{-\gamma_1 - \sqrt{\gamma_1^2 - 4\gamma_0 1/\mu_l}} - \frac{2\gamma_0}{-\gamma_1 - \sqrt{\gamma_1^2 - 4\gamma_0 1/\mu_k}} > 0$$
$$\lambda_{l1} > \lambda_{k1}$$

which completes the proof.

Lemma 3: If $\gamma_0 \neq 0$ and $\mu_l \neq \mu_k$, then there is no positive γ_1 to make $\lambda_{l1}(\gamma_1) = \lambda_{k1}(\gamma_1)$.

Proof (Proof by Contradiction): Assume that $\gamma_1 > 0$ is available to make $\lambda_{l1}(\gamma_1) = \lambda_{k1}(\gamma_1)$.

$$-\gamma_1\mu_l + \sqrt{(\gamma_1\mu_l)^2 - 4\gamma_0\mu_l} = -\gamma_1\mu_k + \sqrt{(\gamma_1\mu_k)^2 - 4\gamma_0\mu_k}$$

Transpose the terms and calculate the square of the obtained equation:

$$(\gamma_1\mu_k - \gamma_1\mu_l)^2 = \left(\sqrt{(\gamma_1\mu_k)^2 - 4\gamma_0\mu_k} - \sqrt{(\gamma_1\mu_l)^2 - 4\gamma_0\mu_l}\right)^2$$
$$\gamma_1^2\mu_l\mu_k - 2\gamma_0(\mu_l + \mu_k) = \sqrt{(\gamma_1\mu_k)^2 - 4\gamma_0\mu_k} \times \sqrt{(\gamma_1\mu_l)^2 - 4\gamma_0\mu_l}$$
$$\left(\gamma_1^2\mu_l\mu_k - 2\gamma_0(\mu_l + \mu_k)\right)^2 = \left(\sqrt{(\gamma_1\mu_k)^2 - 4\gamma_0\mu_k} \times \sqrt{(\gamma_1\mu_l)^2 - 4\gamma_0\mu_l}\right)^2$$
$$\gamma_0^2(\mu_l - \mu_k)^2 = 0 \tag{8}$$

By (8), it is apparent that $\mu_l = \mu_k$ which is disagree with precondition $\mu_l \neq \mu_k$, thus we have the desired result.

For a given γ_1,

1) If $\gamma_1^2\mu_n^2 - 4\gamma_0\mu_n \leq 0$, then $\gamma_0 \geq \frac{\gamma_1^2\mu_n}{2}$.

On the basis of Lemma 1 and Lemma 3, it can be seen that, if the eigenvalues of H satisfy

$$\mu_n \geq \mu_{n-1} \geq \cdots \geq \mu_2 \geq \mu_1 > 0,$$

then

$$c(\gamma_1) = -\max\{Re\lambda_{i1}, i = 1, 2, \ldots, n\} = \frac{\gamma_1\mu_1}{2}.$$

2) If $\gamma_1^2\mu_n^2 - 4\gamma_0\mu_n > 0$ and $\gamma_1^2\mu_1^2 - 4\gamma_0\mu_1 < 0$, then

$$\frac{\gamma_1^2\mu_1}{4} < \gamma_0 < \frac{\gamma_1^2\mu_n}{4}.$$

On the basis of Lemma 2, if λ_{i1} is a real number, the value of λ_{i1} gets bigger with the increase of μ_i, which leads to the increasing distance from the imaginary axis. As the value of γ_0 increased, velocity of λ_{11} along the root locus becomes the fastest, whereas velocity of λ_{11} tends to be the slowest. Lemma 3 shows that if the eigenvalues of H are different, there is no converging point of the root loci of the corresponding λ_{i1}.

Notice that:

$$c(\gamma_1) = -\max\{Re\lambda_{11}, Re\lambda_{n1}\} = -\max\left\{-\frac{\gamma_1\mu_1}{2}, \frac{-\gamma_1\mu_n+\sqrt{\gamma_1^2\mu_n^2-4\gamma_0\mu_n}}{2}\right\}$$

Let

$$-\frac{\gamma_1\mu_1}{2} = \frac{-\gamma_1\mu_n+\sqrt{\gamma_1^2\mu_n^2-4\gamma_0\mu_n}}{2},$$

then we have:

$$\gamma_0 = \frac{2\mu_1\mu_n\gamma_1^2-\mu_1^2\gamma_1^2}{4\mu_n}.$$

If $\frac{\gamma_1^2\mu_1}{4} < \gamma_0 \le \frac{2\mu_1\mu_n\gamma_1^2-\mu_1^2\gamma_1^2}{4\mu_n}$, then

$$c(\gamma_1) = \frac{\gamma_1\mu_n-\sqrt{\gamma_1^2\mu_n^2-4\gamma_0\mu_n}}{2}.$$

If $\frac{2\mu_1\mu_n\gamma_1^2-\mu_1^2\gamma_1^2}{4\mu_n} < \gamma_0 < \frac{\gamma_1^2\mu_n}{4}$, then $c(\gamma_1) = \frac{\gamma_1\mu_1}{2}$.

3) If $\gamma_1^2\mu_1^2 - 4\gamma_0\mu_1 \ge 0$ (i.e. $0 < \gamma_0 \le \frac{\gamma_1^2\mu_1}{4}$), then

$$c(\gamma_1) = \frac{\gamma_1\mu_n-\sqrt{\gamma_1^2\mu_n^2-4\gamma_0\mu_n}}{2}.$$

In conclusion, if $0 < \gamma_0 \le \frac{2\mu_1\mu_n\gamma_1^2-\mu_1^2\gamma_1^2}{4\mu_n}$, and then $c(\gamma_1) = \frac{\gamma_1\mu_n-\sqrt{\gamma_1^2\mu_n^2-4\gamma_0\mu_n}}{2}$. It is clear that $c(\gamma_1)$ is the increasing function of γ_0, and it can improve the exponential convergence rate by increasing the value of γ_0. If $\gamma_0 > \frac{2\mu_1\mu_n\gamma_1^2-\mu_1^2\gamma_1^2}{4\mu_n}$, and then $c(\gamma_1) = \frac{\gamma_1\mu_1}{2}$, which means that γ_0 does not affect the exponential convergence rate. Specially, if $\gamma_0 = \frac{2\mu_1\mu_n\gamma_1^2-\mu_1^2\gamma_1^2}{4\mu_n}$ (i.e. $Re\lambda_{11} = \lambda_{n1}$), the system achieves the maximum convergence speed.

B. THE INFLUENCES OF γ_1 ON THE MAXIMUM CONVERGENCE RATE

For a given γ_0, the results will be presented in the sequel which can be worked out in a similar process to Section 2.1.

If $0 < \gamma_1 \le \frac{2\sqrt{\gamma_0\mu_n}}{\sqrt{\mu_1(2\mu_n-\mu_1)}}$, and then $c(\gamma_1) = \frac{\gamma_1\mu_1}{2}$, which illustrates that increasing γ_1 can improve the exponential convergence rate. If $\gamma_1 > \frac{2\sqrt{\gamma_0\mu_n}}{\sqrt{\mu_1(2\mu_n-\mu_1)}}$, it implies that $c(\gamma_1)$ is the decreasing function of γ_1, i.e., it will reduce the exponential convergence rate by raising the value of γ_0. Particularly, if $\gamma_1 = \frac{2\sqrt{\gamma_0\mu_n}}{\sqrt{\mu_1(2\mu_n-\mu_1)}}$, the system will achieve the maximum convergence rate.

To summarize above analysis, we have our first main result in this paper as follows.

Theorem 1: Assume that communication topology G is a connected graph and the eigenvalues of H can be written as $\mu_n \ge \mu_{n-1} \ge \cdots \ge \mu_2 \ge \mu_1 > 0$. For a given $\gamma_0 > 0$, if

$$\gamma_1 = \frac{2\sqrt{\gamma_0\mu_n}}{\sqrt{\mu_1(2\mu_n-\mu_1)}}, \quad \gamma_1 \in (0, \infty)$$

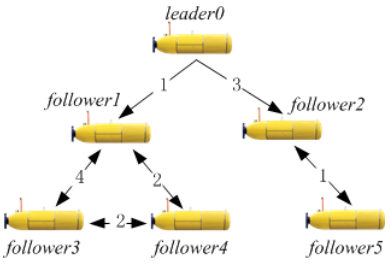

FIGURE 1. Schematic diagram of collaborative navigation systems.

TABLE 1. Initial state of AUVs.

Member	*Position* (m)	*Velocity* (m/s)
Leader 0	(20, 360, 100)	(4, 2, 0)
Follower 1	(80, 350, -10)	(6, 0, -2)
Follower 2	(280, 150, 10)	(0, -5, 1)
Follower 3	(320, -240, -20)	(-3, 7, 2)
Follower 4	(-50, -340, 0)	(2, 3, -2)
Follower 5	(-100, 420, -20)	(5, -6, 2)

then the multi-AUV systems have the maximum convergence rate with an exponential decay e^{-at}, and

$$a = \frac{\gamma_1\mu_1}{2} = \sqrt{\frac{\gamma_0\mu_1\mu_n}{2\mu_n-\mu_1}}.$$

From the above discussion, we can see that the maximum convergence rate is influenced by the maximum or the minimum eigenvalue of H, while the maximum or the minimum eigenvalue of H is decided by the topological structure of the whole multi-AUV systems. Hence, reasonable design of topologies plays an essential role in controlling systems to attain the maximum convergence rate.

C. THE SIMULATIONS AND ANALYSIS OF THE INFLUENCES OF CONTROL GAINS

Assume that there are 6 members in the collaborative navigation systems as shown in Fig. 1 and let node 0 indicate a leader and node1 - node 5 represent 5 followers. The initial state of AUVs in the x, y, z direction is shown in Table 1. The attitude of AUVs is not considered in the simulations, such as roll angle, pitch angle and yaw angle. The total number of loops and the simulation time are set to 5000 and 50s respectively.

As shown in Fig. 1, the adjacency matrix A and Laplacian L of topology G_{ff} between followers, and matrix D and matrix H related with relationship between leader and followers are obtained as:

$$A = \begin{bmatrix} 0 & 0 & 4 & 2 & 0 \\ 0 & 0 & 0 & 0 & 1 \\ 4 & 0 & 0 & 2 & 0 \\ 2 & 0 & 2 & 0 & 0 \\ 0 & 1 & 0 & 0 & 0 \end{bmatrix}$$

$$D = \begin{bmatrix} 1 & & & & \\ & 3 & & & \\ & & 0 & & \\ & & & 0 & \\ & & & & 0 \end{bmatrix}$$

$$L = \begin{bmatrix} 6 & 0 & -4 & -2 & 0 \\ 0 & 1 & 0 & 0 & -1 \\ -4 & 0 & 6 & -2 & 0 \\ -2 & 0 & -2 & 4 & 0 \\ 0 & -1 & 0 & 0 & 1 \end{bmatrix}$$

$$H = \begin{bmatrix} 7 & 0 & -4 & -2 & 0 \\ 0 & 4 & 0 & 0 & -1 \\ -4 & 0 & 6 & -2 & 0 \\ -2 & 0 & -2 & 4 & 0 \\ 0 & -1 & 0 & 0 & 1 \end{bmatrix}$$

The eigenvalues of the matrix is calculated as 10.5367, 6.1549, 4.3028, 0.6972 and 0.3084 in a descending order.

Case 1: Let $\gamma_0 = 0.5$. When $\gamma_1 = 1.814$, the maximum convergence rate is obtained by calculation and $c(\gamma_1) = 0.2797$. The simulation result is shown in Fig. 2.

Case 2: Let $\gamma_0 = 0.5$ and $\gamma_1 = 3$. The simulation result is shown in Fig. 3.

Case 3: Let $\gamma_0 = 2$ and $\gamma_1 = 1.814$. The simulation result is shown in Fig. 4.

Case 4: Let $\gamma_0 = 0.1$ and $\gamma_1 = 1.814$. The simulation result is shown in Fig. 5.

As can be seen from the simulation results, the time that the state of followers converges to that of leader is 20s, 30s, 20s and 90s respectively. Comparing Fig. 2 with Fig. 3, we can see that the convergence rate decreases with the increase of γ_1 in the case of a fixed γ_0 and $\gamma_1 > 1.814$. From Fig. 2, Fig. 4 and Fig. 5, we observe that the convergence rate enhances with the raise of γ_0, if $\gamma_0 < 0.5$ and γ_1 is given. Moreover, if $\gamma_0 > 0.5$, γ_0 has no effects on the convergence rate but exacerbates volatility as shown in Fig. 2.

III. THE INFLUENCES OF NETWORK TOPOLOGY ON CONVERGENCE RATE

A. THE INFLUENCES OF GRAPH CONNECTIVITY ON CONVERGENCE RATE TO CONSENSUS

In [22], the convergence analysis of a linear consensus protocol was provided under different situations. For the strongly connected, balanced and fixed digraph of first-order integrators, with the aid of a valid Lyapunov function, the defined group disagreement vector was proofed to vanish globally asymptotically with a speed which was equal to the Fiedler eigenvalue of the mirror graph of original topology. This established a connection between the convergence rate of a linear consensus protocol and the algebraic connectivity of the network. Then, the conclusion was extended to the network with switching information flow. An average-consensus was reached and the group disagreement vector vanished exponentially fast with a rate which was the same with the least algebraic connectivity. The convergence analysis of the discrete-time consensus protocol was almost identical to its continuous-time counterpart [23]. A discrete-time consensus was globally exponentially achieved with a minimum velocity that was equal to the second largest eigenvalue of the symmetric part of the Perron matrix for the connected

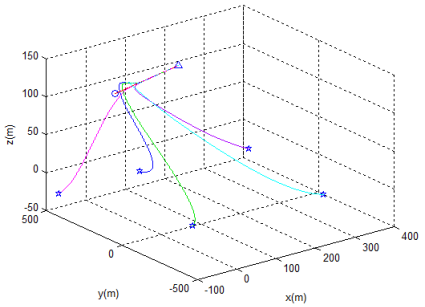

(a)

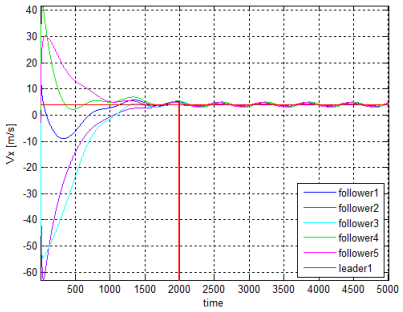

(b)

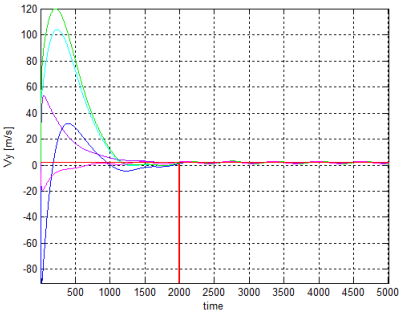

(c)

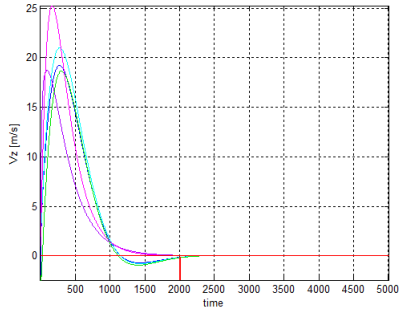

(d)

FIGURE 2. Trajectory and velocity curves with $\gamma_0 = 0.5$, $\gamma_1 = 1.814$. (a) Motion track in 3*D* space. (b) Velocity variation in *x* axis. (c) Velocity variation in *y* axis. (d) Velocity variation in *z* axis.

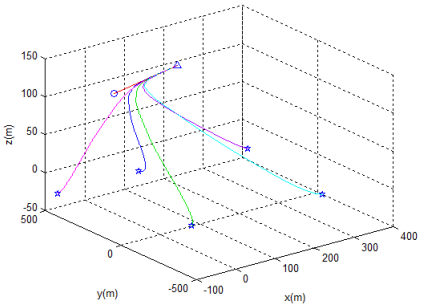

(a)

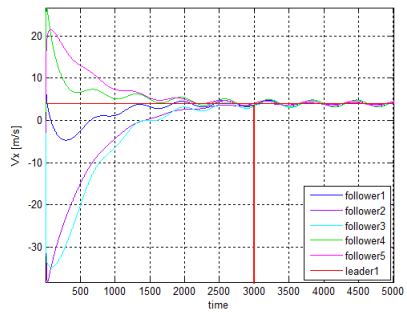

(b)

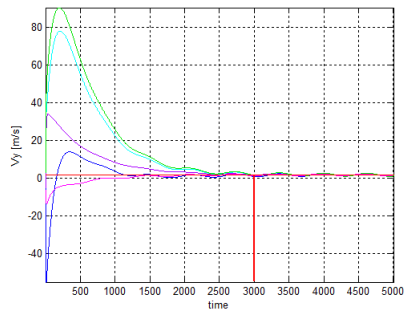

(c)

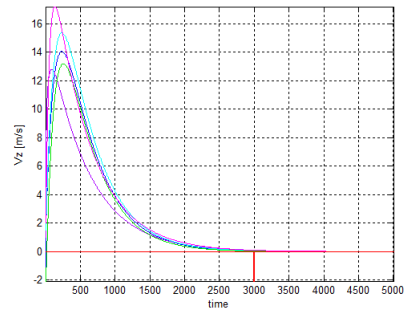

(d)

FIGURE 3. Trajectory and velocity curves with $\gamma_0 = 0.5$, $\gamma_1 = 3$. (a) Motion track in 3*D* space. (b) Velocity variation in *x* axis. (c) Velocity variation in *y* axis. (d) Velocity variation in *z* axis.

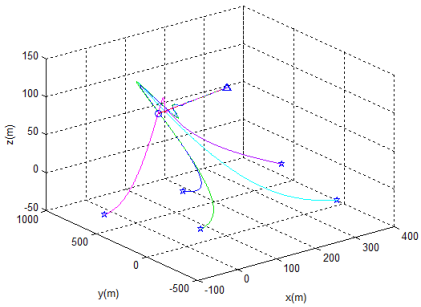

(a)

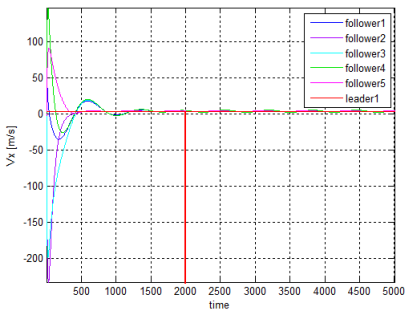

(b)

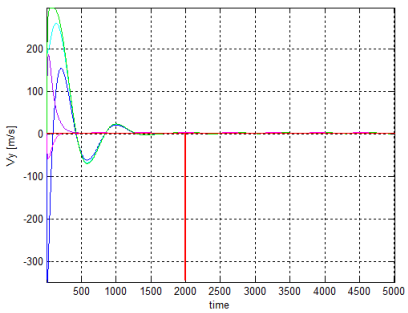

(c)

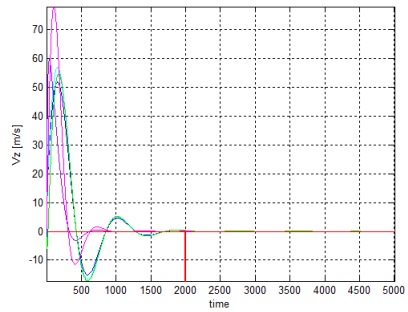

(d)

FIGURE 4. Trajectory and velocity curves with $\gamma_0 = 2$, $\gamma_1 = 1.814$. (a) Motion track in 3*D* space. (b) Velocity variation in *x* axis. (c) Velocity variation in *y* axis. (d) Velocity variation in *z* axis.

undirected network. It means that the issue of convergence rate of consensus algorithm can be transformed into that of the algebraic connectivity of the network topology. As a consequence, how to increase the algebraic connectivity is the key to accelerate convergence. A well-known observation in [24] was that algebraic connectivity was relatively large for dense undirected graphs and relatively small for sparse undirected graphs. For a regular network, the algebraic

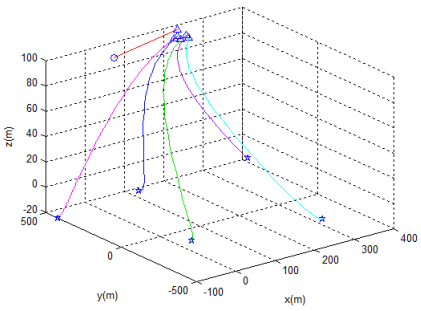

(a)

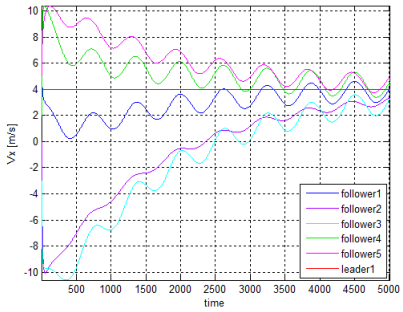

(b)

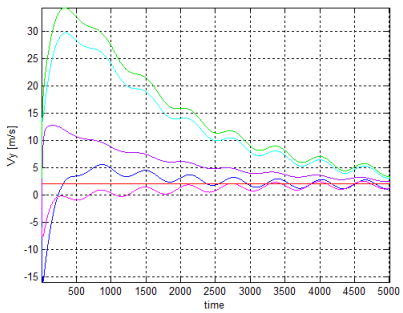

(c)

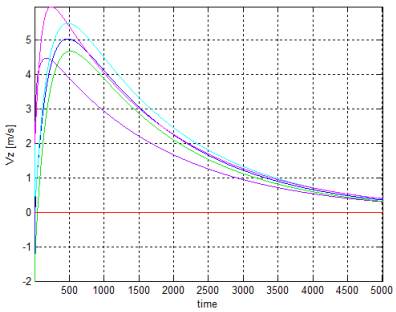

(d)

FIGURE 5. Trajectory and velocity curves with $\gamma_0 = 0.1$, $\gamma_1 = 1.814$. (a) Motion track in 3*D* space. (b) Velocity variation in *x* axis. (c) Velocity variation in *y* axis. (d) Velocity variation in *z* axis.

connectivity could be considerably increased via random rewriting by 1000 times or more without adding new links or nodes to the network [25]. In [26], an iterative greedy-type algorithm was proposed to maximize the second smallest eigenvalue of a state-dependent graph Laplacian in which the weight was a function of the distance between two vertexes. In [27], with some constrains such as a predefined communication cost and time delays on the links, the goal to design an optimal communication topology resulting in the fastest convergence of average consensus was replaced by a mixed integer semi-definite program. It was really an effective way to address this kind of problem. In [28], the convergence conditions of second-order consensus for the directed network with switching topology were specified and the exponential convergence rate was derived by utilizing Lyapunov function method. The majority of recent works focused on networks with identical dynamic equations. Nevertheless, a generalized integrator network, each node of which is a single-integrator cascaded with some heterogeneous non-integrator internal dynamics, was designated in [29]. Based on the Lyapunov analysis, it is possible to derive the worst performance bound of convergence rate to consensus if the interconnection graph is undirected and connected and the non-integrator internal dynamics of each node is strictly passive. Increasing the value of the second smallest eigenvalue of Laplacian matrix was beneficial for the enhancement of convergence rate.

Results in [30] demonstrated that the convergence rate was related not only to algebraic connectivity but also to eigenratio which was denoted by the ratio of the second smallest to the largest eigenvalue of the graph Laplacian. Based on the introduction in [31], the lower bound of the optimal asymptotic convergence factor for consensus of linear discrete-time multi-agent systems was deduced, which was the evaluation of convergence rate. Furthermore, similar results were extended to second-order consensus. In [32], group diameter was introduced to measure the scale of the entire multi-agent systems. The interaction between agents induced a series of movements toward the center of group for the purpose of consensus. In this case, group diameter vanished when agents tended to coincide with each other. Under the assumptions of persistent connectivity of the interaction graph and of slow divergence of reciprocal interaction weights, the estimation of convergence rate was proofed to expand the conclusions in [33]. Reference [34] proved that convergence rate explicitly depended on the diameter of the persistent graph in a social network. Other similar analyses were presented in [35]–[39] to characterize the bound of convergence rate of consensus evolution. In this paper, with the aid of the root locus chart which depicts the positions of eigenvalues of graph Laplacian, the specific form of the exponential convergent rate is derived rather than simply a lower bound.

Now we are ready to present our next main result in this paper on leader-following architecture under undirected topology based on the effects in [40] and [41].

Theorem 2: If the topology between followers is undirected, then the speed of consensus, with a given γ_1, will be accelerated by adding undirected edges in the topology formed with followers or adding directed edges in the

topology formed with followers and leaders or increasing the weights on the communication links.

Proof: After adding undirected edges in the topology formed with followers or adding directed edges in the topology formed with followers and leaders or increasing the weights on the communication links, the established matrix H_1 is equivalent to the sum of the original matrix H and a symmetrical matrix with nonnegative eigenvalues.

By Wey1 theorem in [42],

$$\lambda_{\min}(H_1) \geq \lambda_{\min}(H) + \lambda_{\min}(M)$$

Since M has at least one zero eigenvalue and the rest eigenvalues are positive, the inequality $\lambda_{\min}(H_1) \geq \lambda_{\min}(H)$ always holds. With a given γ_1, the maximum convergence rate is proportional to the minimum eigenvalue, thus the maximum convergence increases. The proof is completed.

B. THE INFLUENCES OF WEIGHTS ON CONVERGENCE RATE TO CONSENSUS

The limitations of communication distance and blocking result in the consistent amount of information for each agent in multi-agent systems, in this case, it is essential to discuss weights on the communication links which represent the number and quality of obtained information. How to distribute the weights to achieve a better consistency becomes a hot and important issue.

The work in [31] considered how to find weight matrix in a given network topology to make convergence as fast as possible. For this purpose, two parameters, called asymptotic convergence factor and per-step convergence factor, were defined as measurements of the convergence rate. Moreover, fastest distributed linear averaging problem was formulated as the spectral radius minimization and the spectral norm minimization respectively. Both of them were semi-defined programs in terms of symmetric edge weights. In addition, several examples showed that above optimization procedures were generally substantially faster than the heuristics on the basis of algebra properties of topological graph. In [43], for the problem of parameter estimation in sensor networks, the distributed estimation fusion algorithm based on consensus-average was introduced. In order to accelerate the convergence rate of the improved distributed iterative scheme, an adaptive weight matrix modification method was proposed, in which weight matrix was modified by the steepest descent method. In [44], the proper asymmetric interaction strategies with time-varying weights on links were proposed to accelerate the convergence rate of distributed consensus algorithm. Furthermore, relative results were applied in fluid mixing problems. In [45], a primal-dual distributed algorithm was devised to solve the convex feasibility problem where weights on communication links were interpreted as dual variables. Based on this novel conceptual substitution, weights were updated utilizing arguments from duality theory. Moreover, the convergence of this protocol was faster than some existing methods. Efforts have been made in [46] analyzed the optimization of weights on communication links for consensus method under spatially correlated random topologies. Simulation results revealed that using the link quality estimates and link corrections in the consideration of weights could accelerate the convergence speed to consistency. A thorough investigation of enhancing consensus in weighted network with coupling time-delay was exhibited in [47]. In the proposed consensus protocol based on a weighted Vicsek model, weights were adjusted according to the state incoherence instead of utilizing topological information to suppress the heterogeneity in state in order to obtain an improved convergence efficiency. It is shown in [48] that the ways to choose asymmetric weights were designed to improve the convergence rate of distributed consensus for lattice graphs, 2-dimensional geometric graphs respectively.

Based on above analysis and discussions, we are in a position to present the following main result.

Theorem 3: Assume that the topology between followers is undirected and the parameter γ_0 is given. Then, changing the quantities or weights of communication links, and the maximum convergence will increase, if the ratio of the maximum and the minimum eigenvalues of H decreases.

C. THE INFLUENCES OF HIERARCHICAL STRUCTURE ON CONVERGENCE RATE TO CONSENSUS

A new approach to speed up the convergence was proposed based on the hierarchical graph. In [49], network was divided into several layers and containment control algorithm was designed to make each child layer located in the convex hull of its parent layer. Researches showed that the maximum convergence rate was achieved when the number of layers was close to a constant value with respect to the total number of agents in the network. In [50], a novel hierarchical control strategy was discussed in which the whole graph was decomposed into several connected sub-graphs. The relation between the layers was established by the leader node. Consensus control was performed starting with the lowest layer and moving upwards when the precision error was less than a given value. In this proposed method, faster convergence rate could be obtained because the second smallest eigenvalues of sub-graphs were larger than that in the graphs based on the standard consensus algorithm.

Due to space constraints, the simulations of the influences of topology on convergence rate are not revealed in this paper.

IV. THE CONSENSUS-UPF ALGORITHM FOR COOPERATIVE LOCALIZATION

Since acoustic waves can propagate a few thousand metres under the water with rarely obvious attenuation, underwater collaborative navigation based on acoustic localization becomes mainstream. Nonetheless, multipath effects exist when acoustic waves propagate. Affected by the factors such as salinity, temperature and turbidity of sea water, the effective range and transmission rate of acoustic waves will change. The reflection of acoustic waves will happen when encountering obstacles or vegetation in the seawater, which will result in many nonlinear noises in the measurements of

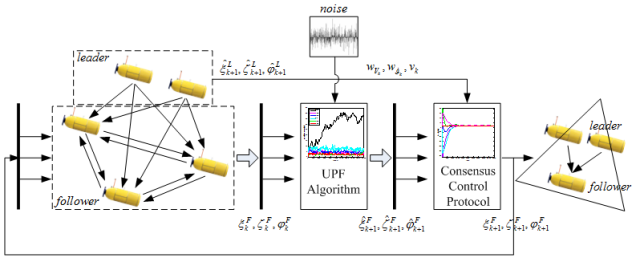

FIGURE 6. The basic schematic of the consensus-UPF algorithm.

sensors installed on the AUVs. That is to say, there is a deviation between the estimated position and the real position. In order to get the positions of AUVs accurately, it is necessary to carry on filtering to measurements and estimate positions. Some filtering algorithms' characteristics are detailed in our previous work [51].

In this paper, we replace the dead reckoning in the consensus algorithm with the movement based on UPF algorithm so that accumulative errors will be eliminated eventually. In the process of each update of the modified algorithm, the key information of each follower is filtered and information fusion based on consensus algorithm is completed by using the estimated state as shown in Fig. 6. The detailed steps are introduced in Section 4.1.

A. COLLABORATIVE NAVIGATION ALGORITHM BASED ON CONSENSUS-UPF

Step 1 (Filter Model): In the noise circumstance, the kinematic equation is described by:

$$\begin{cases} x_{k+1} = x_k + T\left(V_k + w_{V_k}\right)\cos\left(\theta_k\right) \\ y_{k+1} = y_k + T\left(V_k + w_{V_k}\right)\sin\left(\theta_k\right) \\ \theta_{k+1} = \theta_k + T\left(\dot{\theta}_k + w_{\dot{\theta}_k}\right) \end{cases} \tag{9}$$

where (x_k, y_k) and θ_k represent the position and the yaw angle at time t_k respectively. V_k and $\dot{\theta}_k$ indicate forward speed and yaw rate, while T is the estimated time. In addition, w_{V_k} and $w_{\dot{\theta}_k}$ are non-additive noises.

Assume that the collaborative localization framework has two leaders. The measurement is selected as slant range and the measurement equation is defined as:

$$Z_{k+1} = \begin{bmatrix} \sqrt{\left(x^L_{1,k+1} - x^F_{k+1}\right)^2 + \left(y^L_{1,k+1} - y^F_{k+1}\right)^2} + v_{k+1} \\ \sqrt{\left(x^L_{2,k+1} - x^F_{k+1}\right)^2 + \left(y^L_{2,k+1} - y^F_{k+1}\right)^2} + v_{k+1} \end{bmatrix} \tag{10}$$

where $\left(x^F_{k+1}, y^F_{k+1}\right)$ and $\left(x^L_{i,k+1}, y^L_{i,k+1}\right)$ $(i = 1, 2)$ express the coordinates of follower and leader. It is easy to see that measurement noise v_{k+1} is additive.

Step 2 (Parameter Initialization): Sample n particles with initial state $X_0^{(i),F}$ and priori probability density $P_0^{(i),F}$. Associated weight $\tilde{w}_0^{(i),F} = 1/n$. Expand the state and covariance matrices as:

$$X_k^{a(i),F} = \begin{bmatrix} E\left(X_k^{(i),F}\right) \\ w_k \\ v_k \end{bmatrix}$$

$$P_k^{a(i),F} = \begin{bmatrix} P_k^{(i),F} & 0 & 0 \\ 0 & Q_k & 0 \\ 0 & 0 & R_k \end{bmatrix}, \quad i = 1, 2, \cdots, n$$

where w_k and v_k are the process noise and measurement noise respectively, Q_k and R_k are their covariance matrices.

Calculate the σ point set of the i-th particle as follows:

$$\chi_{(0),k}^{a(i),F} = X_k^{a(i),F}$$

$$\chi_{(j),k}^{a(i),F} = X_k^{a(i),F} + \left(\sqrt{(L+\lambda)P_k^{a(i),F}}\right)_j \quad (j = 1, 2, \cdots, L)$$

$$\chi_{(j),k}^{a(i),F} = X_k^{a(i),F} - \left(\sqrt{(L+\lambda)P_k^{a(i),F}}\right)_{(j-L)} \quad (j = L+1, L+2, \cdots, 2L)$$

where

$$\chi_{(j),k}^{a(i),F} = \begin{bmatrix} \chi_{(j),k}^{X(i),F} \\ \chi_{(j),k}^{w(i),F} \\ \chi_{(j),k}^{v(i),F} \end{bmatrix}$$

Step 3 (Update the State and Measurement Information of Each σ Point): Sample the external input

$$u_k^{(i),F} = \left[V_k^{(i),F} \;\; \dot{\theta}_k^{(i),F}\right]^T$$

and then transform each σ point's state by (9), i.e., one-step-ahead prediction can be written as:

$$\chi_{(j),k+1|k}^{X(i),F} = f(\chi_{(j),k}^{X(i),F}, u_k^{(i),F} + \chi_{(j),k}^{w(i),F}) \quad (i = 1, 2, \ldots, nj = 0, 1, \ldots, 2L)$$

Mean and covariance matrices of above parameter are calculated as:

$$\bar{\chi}_{k+1/k}^{X(i),F} = \sum_{j=0}^{2L} W_j^{(m)} \chi_{(j),k+1/k}^{X(i),F}$$

$$P_{k+1/k}^{(i),F} = \sum_{i=0}^{2L} W_j^{(c)} (\chi_{(j),k+1/k}^{X(i),F} - \bar{\chi}_{k+1/k}^{X(i),F})(\chi_{(j),k+1/k}^{X(i),F} - \bar{\chi}_{k+1/k}^{X(i),F})^T$$

where

$$W_0^{(m)} = \frac{\lambda}{L+\lambda}$$

$$W_0^{(c)} = \frac{\lambda}{L+\lambda} + 1 - \alpha^2 + \beta$$

$$W_j^{(m)} = W_j^{(c)} = \frac{1}{2(L+\lambda)}, \quad j = 1, 2, \cdots, 2L$$

λ is scale factor, and $\lambda = \alpha^2(L+\kappa) - L$. α determines the spread of σ points around $\bar{\chi}_{k+1/k}^{X(i),F}$. κ is usually set to 0 or $3-L$. β is used to incorporate prior knowledge of the distribution of state.

One-step-ahead prediction of measurement is deduced by (10):

$$Z^{(i)}_{(j),k+1|k} = g(\chi^{X(i),F}_{(j),k+1/k}, X^{L}_{k+1}) + \chi^{v(i),F}_{(j),k+1}$$

Mean, covariance and gain matrices of one-step-ahead prediction are calculated as:

$$\bar{Z}^{(i)}_{k+1} = \sum_{j=0}^{2L} W^{(m)}_j Z^{(i)}_{(j),k+1|k}$$

$$P^{(i)ZZ}_{k+1} = \sum_{j=0}^{2L} W^{(c)}_j (Z^{(i)}_{(j),k+1|k} - \bar{Z}^{(i)}_{k+1})(Z^{(i)}_{(j),k+1|k} - \bar{Z}^{(i)}_{k+1})^T$$

$$P^{(i),ZX}_{k+1} = \sum_{j=0}^{2L} W^{(c)}_j (\chi^{X(i),F}_{(j),k+1/k} - \bar{\chi}^{X(i),F}_{k+1/k})(Z^{(i)}_{(j)k+1|k} - \bar{Z}^{(i)}_{k+1})^T$$

$$K^{(i)}_{k+1} = P^{(i),ZX}_{k+1}\left(P^{(i),ZZ}_{k+1}\right)^{-1}$$

The state and covariance matrices are updated as:

$$\bar{X}^{X(i),F}_{k+1} = \bar{\chi}^{X(i),F}_{k+1/k} + K^{(i)}_{k+1}\left(Z_{k+1} - \bar{Z}^{(i)}_{k+1}\right)$$

$$P^{(i)F}_{k+1} = P^{(i)F}_{k+1,k} - K^{(i)}_{k+1}P^{(i)ZZ}_{k+1}\left(K^{(i)}_{k+1}\right)^T$$

Step 4 (Calculate and Normalize the Weights): The n particles are regenerated and then the weights are updated as follows:

$$w^{(i),F}_{k+1} = w^{(i),F}_{k} \frac{p(Z_{k+1}\left|X^{(i),F}_{k+1}\right.)p(X^{(i),F}_{k+1}\left|X^{(i),F}_{k}\right.)}{q\left(X^{(i),F}_{k+1}\left|X^{(i),F}_{0:k}\right., Z_{1:k+1}\right)}$$

where $p(Z_{k+1}\left|X^{(i),F}_{k+1}\right.)$ and $p(X^{(i),F}_{k+1}/X^{(i),F}_{k})$ are likelihood probability and priori probability which are influenced by measurement and system equations respectively.

$$q\left(X^{(i),F}_{k+1}\left|X^{(i),F}_{0:k}\right., Z_{1:k+1}\right)$$

is called importance density function, and

$$q\left(X^{(i),F}_{k+1}\left|X^{(i),F}_{0:k}\right., Z_{1:k+1}\right) \sim \mathrm{N}\left(\bar{X}^{X(i),F}_{k+1} P^{(i),F}_{k+1}\right).$$

Normalize particle weights as:

$$\tilde{w}^{(i),F}_{k+1} = w^{(i),F}_{k+1}\frac{1}{\sum_{i=1}^{n} w^{(i),F}_{k+1}}$$

Step 5 (Complete the Resampling Procedure): Based on residual resampling algorithm, results of the first sampling can be written with:

$$n^{(i)}_1 = [\![n \cdot \tilde{w}^{(i),F}_{k+1,1}]\!], \quad j = 1, 2$$

$$\tilde{w}^{(i),F}_{k+1,2} = n_2^{-1}\left(\tilde{w}^{(i),F}_{k+1} n - n^{(i)}_1\right)$$

where n shows the quantity of particles and $[\![\cdot]\!]$ means rounding operation. Notice that $\tilde{w}^{(i),F}_{k+1,2}$ and n_1 are regarded as the updated probability and quantity in the process of second sampling, and $n_1 = \sum_{i=1}^{n} n^{(i)}_1$. $n_2\,(= n - n_1)$ particles are also added to restore the lost fractional part caused by rounding. n_1 and n_2 represent the total particles by reampling, and weight is $1/n$

Step 6 (Obtain the Estimated State and Covariance Matrix):

$$X^{F}_{k+1} = \sum_{i=1}^{n} X^{(i),F}_{k+1}\tilde{w}^{(i),F}_{k+1}$$

$$P^{F}_{k+1} = \sum_{i=1}^{n} \tilde{w}^{(i),F}_{k+1}\left(X^{(i),F}_{k+1} - X^{F}_{k+1}\right)^2$$

Step 7 (Exchange the State by Consensus Protocol): After obtaining the filtered movement information, as to the selected follower, the corresponding state of leaders and neighbors is utilized to update follower's current state by (2).

B. THE SIMULATIONS OF CONSENSUS-UPF ALGORITHM AND THE INFLUENCES OF TOPOLOGY

In simulation study, we concentrate on the topology shown in Fig. 7 (a). Assigning that node 0 - node 1 represent leaders and node 2 - node 4 are on behalf of followers, and the figures on the edges represent the weights. For each leader, the velocity is constant, which means that the accelerated velocity is zero. Thus the consensus protocol is simplified as (11). After obtaining the filtered positions of followers, (11) is used to exchange the positional information.

$$\begin{aligned}\dot{\xi}^{F}_{i} = &-\sum_{j=1,j\in G_{ff}}^{3} a_{ij}\gamma_0\left(\xi^{F}_{i} - \xi^{F}_{j}\right) \\ &- d_{i1}\gamma_0\left(\xi^{F}_{i} - \xi^{L}_{1}\right) - d_{i2}\gamma_0\left(\xi^{F}_{i} - \xi^{L}_{2}\right) \end{aligned} \quad (11)$$

The matrix form of (11) is rewritten as:

$$\begin{bmatrix}\dot{\xi}^{F}_{1}(t)\\ \dot{\xi}^{F}_{2}(t)\\ \dot{\xi}^{F}_{3}(t)\end{bmatrix} = \gamma_0\Theta_1\begin{bmatrix}\xi^{F}_{1}(t)\\ \xi^{F}_{2}(t)\\ \xi^{F}_{2}(t)\end{bmatrix} + \gamma_0\begin{bmatrix}d_{11} & d_{12}\\ d_{21} & d_{22}\\ d_{31} & d_{32}\end{bmatrix}\begin{bmatrix}\xi^{L}_{1}(t)\\ \xi^{L}_{2}(t)\end{bmatrix}$$

where

$$\Theta_1 = -L - \begin{bmatrix}d_{11} & & \\ & d_{21} & \\ & & d_{31}\end{bmatrix} - \begin{bmatrix}d_{12} & & \\ & d_{22} & \\ & & d_{32}\end{bmatrix}.$$

Then, (12) is discretized into:

$$\begin{bmatrix}\xi^{F}_{1}(kT+T)\\ \xi^{F}_{2}(kT+T)\\ \xi^{F}_{3}(kT+T)\end{bmatrix} = \gamma_0 e^{\Theta_1 T}\begin{bmatrix}\xi^{F}_{1}(kT)\\ \xi^{F}_{2}(kT)\\ \xi^{F}_{2}(kT)\end{bmatrix} + \gamma_0\int_{kT}^{kT+T} e^{\Theta_1(kT+T-\tau)}d\tau\begin{bmatrix}d_{11} & d_{12}\\ d_{21} & d_{22}\\ d_{31} & d_{32}\end{bmatrix}\begin{bmatrix}\xi^{L}_{1}(kT)\\ \xi^{L}_{2}(kT)\end{bmatrix}$$

TABLE 2. Initial state of AUVs.

	$Leader0$	$Leader1$	$Follower2$	$Follower3$	$Follower4$
$Position\ (m)$	(28, 15)	(32, -24)	(2, 36)	(38, -15)	(8, 35)
$Velocity\ (kn)$	1	4	6	5	-3
$Yaw\ angle\ (^\circ)$	90	60	30	36	45
$Sampling\ time\ (s)$		0.01			
$Simulation\ time\ (s)$		10			
$Parameters$		$\alpha = 1,\ \beta = 2,\ \kappa = 0,\ \gamma_0 = 2$			
$The\ number\ of\ Particles$		50			

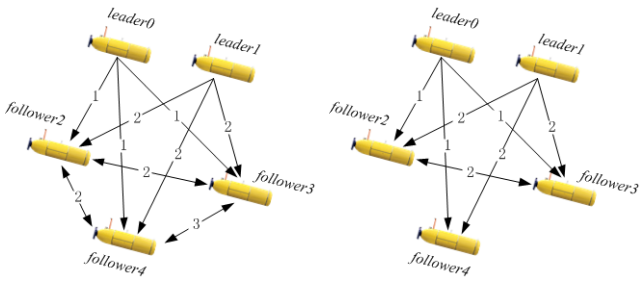

FIGURE 7. Topology of collaborative navigation systems.

TABLE 3. Comparison experiments.

$Algorithm$	$RMSE$	$Follower1$	$Follower2$	$Follower3$
UPF	$Mean$	15.5675	52.7218	7.0408
	$Variance$	5.0600	11.8336	5.8988
$Consensus-UPF$	$Mean$	3.9295	3.8577	3.8447
$(Fig.\ 7\ (b))$	$Variance$	0.2577	0.1933	0.3050
$Consensus-UPF$	$Mean$	3.6939	3.5878	3.5498
$(Fig.\ 7\ (a))$	$Variance$	0.2570	0.1085	0.1919

$$= \gamma_0 e^{\Theta_1 T} \begin{bmatrix} \xi_1^F(kT) \\ \xi_2^F(kT) \\ \xi_2^F(kT) \end{bmatrix} + \gamma_0 \left(\Theta_1^{-1} e^{\Theta_1 T} - \Theta_1^{-1} \right) \begin{bmatrix} d_{11} & d_{12} \\ d_{21} & d_{22} \\ d_{31} & d_{32} \end{bmatrix} \begin{bmatrix} \xi_1^L(kT) \\ \xi_2^L(kT) \end{bmatrix}$$

$$= \gamma_0 e^{\Theta_1 T} \begin{bmatrix} \xi_1^F(kT) \\ \xi_2^F(kT) \\ \xi_2^F(kT) \end{bmatrix} + \gamma_0 \left(\Theta_1^{-1} e^{\Theta_1 T} - \Theta_1^{-1} \right) \begin{bmatrix} d_{11} & d_{12} \\ d_{21} & d_{22} \\ d_{31} & d_{32} \end{bmatrix} \begin{bmatrix} \xi_1^L(kT) \\ \xi_2^L(kT) \end{bmatrix}$$

Assume that noise is Gaussian white noise with zero-mean. Initial parameter settings are shown in Table 2. We intend to change the topology, specifically, to remove the connections between node 2 and node 4 and between node 3 and node 4 respectively as shown in Fig. 7 (b). The filtering experiment is tested 50 times using consensus-UPF algorithm with topologies revealed in Fig. 7 (a) and Fig. 7 (b). Simulation results are shown in Table 3 and Fig. 8.

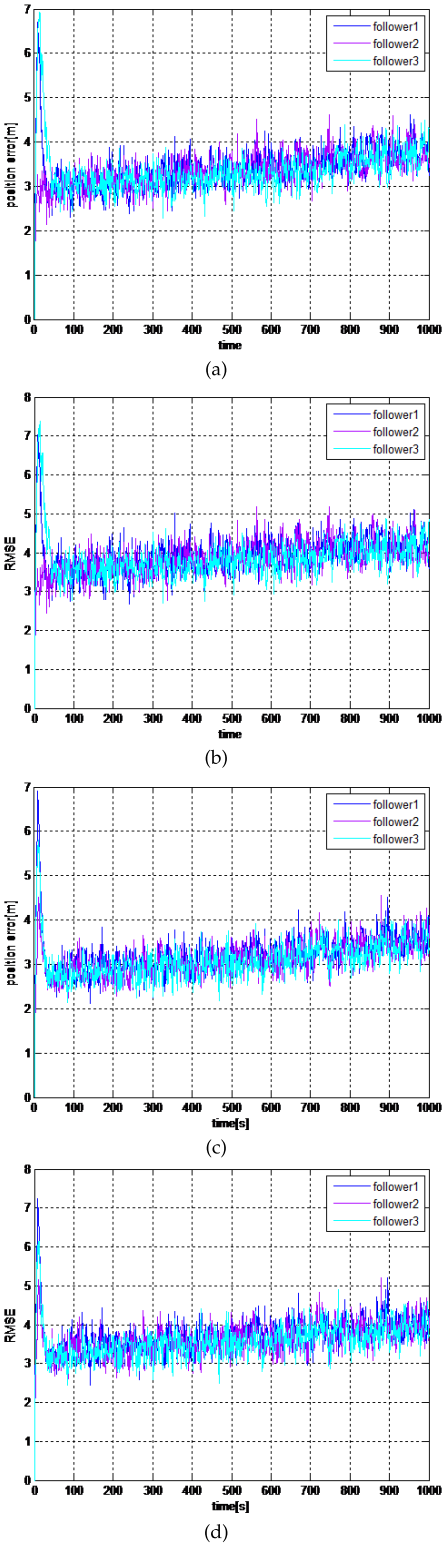

FIGURE 8. Positioning errors and RMSE of the follower.

In this paper, root mean square error (RMSE) is selected to evaluate the localization accuracy.

$$RMSE = \sqrt{\frac{1}{N}\sum_{k=1}^{N}\left(\begin{matrix}\left(x(kT) - \hat{x}(kT)\right)^2 \\ +\left(y(kT) - \hat{y}(kT)\right)^2\end{matrix}\right)}$$

where $(x(kT), y(kT))$ and $(\hat{x}(kT), \hat{y}(kT))$ are the actual and estimated positions of follower. Moreover, N is the experiment time.

Notice that Fig. 8 (a) and Fig. 8 (b) indicate the positioning errors and RMSE related to the topology in Fig. 7 (b), and Fig. 8 (c) and Fig. 8 (d) illustrate the positioning errors and RMSE related to the topology in Fig. 7 (a) respectively. Due to the smaller sampling step in our experiments, the accumulated errors are generated by the larger number of sampling times in the process of dead reckoning in the fixed simulation time. Although the UPF algorithm is able to control the positioning accuracy within a certain range, the filtering effect is poor. As shown in the results, the cooperative navigation and localization approach based on the consensus-UPF algorithm has a higher positioning accuracy than the UPF algorithm, because the key information is exchanged with leaders or neighbor followers in each iteration, which improves the positioning accuracy effectively. Furthermore, the amount of computation is not significantly increased. The consensus-UPF algorithm can not only guarantee the high positioning precision, but also make all the state of followers maintain the same level with leader after a period of time in order to attain consistency. In addition, the better the connectivity of topology is, the more perfect the interactions between AUVs are, and the higher precision the collaborative navigation and localization will have. Thus, it is an advisable method to increase the connectivity of multi-AUV systems for improving the accuracy of collaborative navigation and positioning.

V. CONCLUSIONS

In this work, we have introduced a graph theory model with leader-follower architecture for multi-AUV systems based on second-order consensus protocol. More current developments and contributions on enhancing the convergence rate are discussed, especially for the influences of control gains and network topology. For the sake of eliminating noises during the navigation, a collaborative navigation algorithm based on consensus-UPF algorithm is designed, which is shown to have a perfect filtering effect. Moreover, the influences of topologies imposed on the proposed algorithm are studied. Simulation results are included to illustrate the effectiveness and feasibility of the proposed new design techniques.

REFERENCES

[1] Z. Jin and R. M. Murray, "Multi-hop relay protocols for fast consensus seeking," in *Proc. 45th IEEE Conf. Decision Control*, San Diego, CA, USA, Dec. 2006, pp. 1001–1006.

[2] W. Yang, X. Wang, and H. Shi, "Fast consensus seeking in multi-agent systems with time delay," *Syst. Control Lett.*, vol. 62, no. 3, pp. 269–276, Mar. 2013.

[3] Y. Cao, W. Ren, and Y. Chen, "Multi-agent consensus using both current and outdated states," in *Proc. 17th IFAC World Congr.*, Seoul, South Korea, Jul. 2008, pp. 2874–2879.

[4] J. Li, S. Xu, Y. Chu, and H. Wang, "Distributed average consensus control in networks of agents using outdated states," *IET Control Theory Appl.*, vol. 4, no. 5, pp. 746–758, May 2010.

[5] Y. She and H. Fang, "Fast consensus seeking for multi-agent systems," *Syst. Eng. Electron.*, vol. 22, no. 3, pp. 534–539, Jun. 2011.

[6] P. Shi and Q. Shen, "Cooperative control of multi-agent systems with unknown state-dependent controlling effects," *IEEE Trans. Autom. Sci. Eng.*, vol. 12, no. 3, pp. 827–834, Jul. 2015.

[7] Q. Shen and P. Shi, "Distributed command filtered backstepping consensus tracking control of nonlinear multiple-agent systems in strict-feedback form," *Automatica*, vol. 53, no. 3, pp. 120–124, 2015.

[8] X. Wang, S. Li, and P. Shi, "Distributed finite-time containment control for double-integrator multiagent systems," *IEEE Trans. Cybern.*, vol. 44, no. 9, pp. 1518–1528, Sep. 2014.

[9] H. Du, S. Li, and P. Shi, "Robust consensus algorithm for second-order multi-agent systems with external disturbances," *Int. J. Control*, vol. 85, no. 12, pp. 1913–1928, 2012.

[10] H. Yu, P. Shi, and C.-C. Lim, "Robot formation control in stealth mode with scalable team size," *Int. J. Control*, vol. 89, no. 11, pp. 2155–2168, Mar. 2016, doi: 10.1080/00207179.2016.1149887.

[11] H. Yu, P. Shi, and C.-C. Lim, "Scalable formation control in stealth with limited sensing range," *Int. J. Robust Nonlinear Control*, vol. 27, no. 3, pp. 410–433, 2016, doi: 10.1002/rnc.3579.

[12] Y. Tang, X. Xing, H. R. Karimi, L. Kocarev, and J. Kurths, "Tracking control of networked multi-agent systems under new characterizations of impulses and its applications in robotic systems," *IEEE Trans. Ind. Electron.*, vol. 63, no. 2, pp. 1299–1307, Feb. 2016.

[13] C. Qu, X. Cao, H. R. Karimi, Z. Zhang, and Z. Zhang, "Finite-time distributed energy-to-peak control for uncertain multiagent systems," *Abstract Appl. Anal.*, vol. 2014, Jan. 2014, Art. no. 260201.

[14] Y. Liu, H. R. Karimi, and X. Liu, "Distributed consensus for discrete-time directed networks of multiagents with time-delays and random communication links," *Abstract Appl. Anal.*, vol. 2013, Jun. 2013, Art. no. 158731.

[15] G. Wen, Y. Zhao, Z. Duan, W. Yu, and G. Chen, "Containment of higher-order multi-leader multi-agent systems: A dynamic output approach," *IEEE Trans. Autom. Control*, vol. 61, no. 4, pp. 1135–1140, Apr. 2016.

[16] G. Wen, W. Yu, G. Hu, J. Cao, and X. Yu, "Pinning synchronization of directed networks with switching topologies: A multiple Lyapunov functions approach," *IEEE Trans. Neural Netw. Learn. Syst.*, vol. 26, no. 12, pp. 3239–3250, Dec. 2015.

[17] J. Wang, "Network-based containment control protocol of multi-agent systems with time-varying delays," *Int. J. Innov. Comput., Inf. Control*, vol. 12, no. 6, pp. 2089–2098, Dec. 2016.

[18] J. Song, "Observer-based consensus control for networked multi-agent systems with delays and packet-dropouts," *Int. J. Innov. Comput., Inf. Control*, vol. 12, no. 4, pp. 1287–1302, 2016.

[19] C. K. Ahn, L. Wu, and P. Shi, "Stochastic stability analysis for 2-D Roesser systems with multiplicative noise," *Automatica*, vol. 69, pp. 356–363, Jul. 2016.

[20] C. K. Ahn, P. Shi, and M. V. Basin, "Two-dimensional dissipative control and filtering for Roesser model," *IEEE Trans. Autom. Control*, vol. 60, no. 7, pp. 1745–1759, Jul. 2015.

[21] J. M. Pak, C. K. Ahn, P. Shi, Y. S. Shmaliy, and M. T. Lim, "Distributed hybrid particle/FIR filtering for mitigating NLOS effects in TOA based localization using wireless sensor networks," *IEEE Trans. Ind. Electron.*, to be published, doi: 10.1109/TIE.2016. 2608897.

[22] R. O. Saber and R. M. Murray, "Consensus problem in networks of agents with switching topology and time-delays," *IEEE Trans. Autom. Control*, vol. 49, no. 9, pp. 1520–1533, Sep. 2004.

[23] R. Olfati-Saber, J. A. Fax, and R. M. Murray, "Consensus and cooperation in networked multi-agent systems," *Proc. IEEE*, vol. 95, no. 1, pp. 215–233, Jan. 2007.

[24] C. Godsil and G. Royle, *Algebraic Graph Theory, Graduate Texts in Mathematics*. vol. 27. New York, NY, USA: Springer-Verlag, 2001.

[25] R. O. Saber, "Ultrafast consensus in small-world networks," in *Proc. Amer. Control Conf.*, Portland, OR, USA, Jun. 2005, pp. 2371–2378.

[26] Y. Kim and M. Mesbahi, "On maximizing the second smallest eigenvalue of a state-dependent graph Laplacian," in *Proc. Amer. Control Conf.*, Portland, OR, USA, Jun. 2005, pp. 99–103.

[27] M. Rafiee and A. M. Bayen, "Optimal network topology design in multi-agent systems for efficient average consensus," in *Proc. 49th IEEE Conf. Decision Control*, Atlanta, GA, USA, Dec. 2010, pp. 3877–3883.

[28] J. Qin, H. Gao, and W. X. Zhang, "Second-order consensus for multi-agent systems with switching topology and communication delay," *Syst. Control Lett.*, vol. 60, no. 6, pp. 390–397, 2011.

[29] K.-K. Oh, B.-Y. Kim, H. R. Cha, K. L. Moore, and H.-S. Ahn, "Consensus of generalized integrators: Convergence rate and disturbance attenuation property," *Automatica*, vol. 65, pp. 115–119, Mar. 2016.

[30] K. You and L. Xie, "Network topology and communication data rate for consensusability of discrete-time multi-agent systems," *IEEE Trans. Autom. Control*, vol. 56, no. 10, pp. 2262–2275, Oct. 2011.
[31] L. Xiao and S. Boyd, "Fast linear iterations for distributed averaging," *Syst. Control Lett.*, vol. 53, no. 1, pp. 65–78, 2004.
[32] S. Martin and A. Girard, "Continuous-time consensus under persistent connectivity and slow divergence of reciprocal interaction weights," *SIAM J. Control Optim.*, vol. 51, no. 3, pp. 2568–2584, 2013.
[33] J. M. Hendrickx and J. N. Tsitsiklis, "Convergence of type-symmetric and cut-balanced consensus seeking systems," *IEEE Trans. Autom. Control*, vol. 58, no. 1, pp. 214–218, Jan. 2013.
[34] G. Shi and K. H. Johansson, "The role of persistent graphs in the agreement seeking of social networks," *IEEE J. Sel. Areas Commun.*, vol. 31, no. 9, pp. 595–606, Sep. 2013.
[35] M. Cao, A. S. Morse, and B. D. O. Anderson, "Reaching a consensus in a dynamically changing environment: Convergence rates, measurement delays, and asynchronous events," *SIAM J. Control Optim.*, vol. 47, no. 2, pp. 601–623, 2008.
[36] A. Nedić, A. Olshevsky, A. Ozdaglar, and J. N. Tsitsiklis, "On distributed averaging algorithms and quantization effects," *IEEE Trans. Autom. Control*, vol. 54, no. 11, pp. 2506–2517, Nov. 2009.
[37] A. Olshevsky and J. N. Tsitsiklis, "Convergence speed in distributed consensus and averaging," *SIAM J. Control Optim.*, vol. 48, no. 1, pp. 33–55, 2009.
[38] A. Olshevsky and J. N. Tsitsiklis, "Degree fluctuations and the convergence time of consensus algorithms," in *Proc. 50th IEEE Conf. Decision Control Eur. Control Conf.*, Orlando, FL, USA, Dec. 2011, pp. 6602–6607.
[39] N. R. Chowdhury, S. Sukumar, and N. Balachandran, "Persistence based convergence rate analysis of consensus protocols for dynamic graph networks," *Eur. J. Control*, vol. 29, pp. 33–43, May 2016.
[40] D. Xu, Y. Li, and T. Wu, "Improving consensus and synchronizability of networks of coupled systems via adding links," *J. Phys. A, Math. Gen.*, vol. 382, no. 2, pp. 722–730, 2007.
[41] J. Zhu, "On consensus speed of multi-agent systems with double-integrator dynamics," *J. Linear Algebra Appl.*, vol. 434, no. 1, pp. 294–306, 2011.
[42] X. Zhang, *Matrix analysis and applications* Beijing, China, Tsinghua Univ. Press, 2004.
[43] F. Xi, J. He, and Z. Liu, "Adaptive fast consensus algorithm for distributed sensor fusion," *IEEE Trans. Signal Process.*, vol. 90, no. 5, pp. 1693–1699, May 2010.
[44] S. Sardellitti, M. Giona, and S. Barbarossa, "Fast distributed average consensus algorithms based on advection-diffusion processes," *IEEE Trans. Single Process.*, vol. 58, no. 2, pp. 826–842, Feb. 2010.
[45] I. Necoara, I. Dumitrache, and J. A. K. Suykens, "Fast primal-dual projected linear iterations for distributed consensus in constrained convex optimization," in *Proc. 49th IEEE Conf. Decision Control*, Atlanta, GA, USA, Dec. 2010, pp. 1366–1371.
[46] D. Jakovetic, J. Xavier, and J. M. F. Moura, "Weight optimization for consensus algorithms with correlated switching topology," *IEEE Trans. Signal Process.*, vol. 58, no. 7, pp. 3788–3801, Jul. 2010.
[47] B. Ning, Q. Ren, and J. Zhao, "Enhancing consensus in weighted networks with coupling time-delay," *Phys. A Statist. Mech. Appl.*, vol. 391, no. 11, pp. 3061–3068, 2012.
[48] H. Hao and P. Barooah, "Improving convergence rate of distributed consensus through asymmetric weights," in *Proc. Amer. Control Conf.*, Montreal, QC, Canada, Jun. 2012, pp. 787–792.
[49] M. Ji, M. Egerstedt, G. Ferrari-Trecate, and A. Buffa, "Hierarchical containment control in heterogeneous mobile networks," *Math. Theory Netw. Syst.*, Kyoto, Japan, Jul. 2006, pp. 2227–2231.
[50] M. Epstein, K. M. Lynch, K. H. Johansson, and R. M. Murray, "Using hierarchical decomposition to speed up average consensus," in *Proc. 17th IFAC World Congr.*, Seoul, South Korea, Jul. 2008, pp. 612–618.
[51] Y. Zhao, W. Xing, H. Yuan, and P. Shi, "A collaborative control framework with multi-leaders for AUVs based on unscented particle filter," *J. Franklin Inst.*, vol. 353, no. 3, pp. 657–669, 2016.

WEN XING received the B.S. and M.S. degrees from Harbin Engineering University, in 2013 and 2015, respectively, where she is currently pursuing the Ph.D. degree in control science and engineering. Her research interests include multi-agent systems, collaborative control, and filtering algorithm.

YUXIN ZHAO (SM'16) received the B.S. degree in automation and the Ph.D. degree in navigation guidance and control from Harbin Engineering University, China, in 2001 and 2005, respectively. He completed the post-doctoral research in Control Science and Engineering from the Harbin Institute of Technology, China, in 2008.

From 2004 to 2005, he was a Visiting Scholar with the The State University of New York, USA. From 2012 to 2013, he was a Research Associate with the Centre for Transport Studies, Department of Department of Civil and Environmental Engineering, Imperial College London, London, U.K. In 2001, he joined Harbin Engineering University and was promoted to Professor in 2013. His current research interests include complex hybrid dynamical systems, optimal filtering, multi-objective optimization techniques, and intelligent vehicle navigation systems

Prof. Zhao is the member of the Royal Institute of Navigation, the Senior Member of China Navigation Institute, and the member of the Mission Planning Committee of Chinese Society of Astronautics.

HAMID REZA KARIMI (M'06–SM'09) was born in 1976. He received the B.Sc. degree (Hons.) in power systems from the Sharif University of Technology, Tehran, Iran, in 1998, and the M.Sc. and Ph.D. (Hons.) degrees in control systems engineering from the University of Tehran, Tehran, in 2001 and 2005, respectively.

He is currently a Professor of Applied Mechanics with the Department of Mechanical Engineering, Politecnico di Milano, Milan, Italy. His current research interests include control systems and mechatronics. He is a member of the IEEE Technical Committee on Systems with Uncertainty, the IFAC Technical Committee on Mechatronic Systems, the Committee on Robust Control, and the Committee on Automotive Control. He is also an Editorial Board Member for some international journals, such as the IEEE Transactions on Industrial Electronics, the IEEE Transactions on Circuit and Systems-I: Regular Papers, the IEEE/ASME Transactions on Mechatronics, *I*nformation Sciences, the IEEE Access, *I*FAC-Mechatronics, *N*eurocomputing, *A*sian Journal of Control, *J*ournal of The Franklin Institute, *I*nternational Journal of Control, Automation, and Systems, *I*nternational Journal of Fuzzy Systems, *I*nternational Journal of e-Navigation and Maritime Economy, *J*ournal of Systems and Control Engineering, and *J*ournal of Control and Decision. He is the 2016 Web of Science Highly Cited Researcher in Engineering.